



# Laboratory earthquakes along faults with a low velocity zone: Directionality and pulse-like ruptures



Kaiwen Xia<sup>a,b,\*</sup>, Ares J. Rosakis<sup>c</sup>

<sup>a</sup> State Key Laboratory of Hydraulic Engineering Simulation and Safety, School of Civil Engineering, Tianjin University, Tianjin 300072, China

<sup>b</sup> Department of Civil and Mineral Engineering, University of Toronto, Toronto, ON, Canada M5S 1A4

<sup>c</sup> Graduate Aerospace Laboratories, California Institute of Technology, Pasadena, CA 91125, USA

## ARTICLE INFO

### Article history:

Received 7 February 2021

Received in revised form 3 April 2021

Accepted 6 April 2021

Available online 19 April 2021

### Keywords:

Earthquake rupture

Low velocity zone

Generalized Rayleigh wave speed

Crack-like rupture

Pulse-like rupture

Supershear speed

## ABSTRACT

Low velocity zone (LVZ) is a common structural feature in geological faults. To examine the effect of LVZ on faulting, a laboratory fault model considering the LVZ is constructed and loaded to different levels. Subsequently ruptures are triggered on one of its contact boundaries with the host rock. The bilateral rupture propagation along this laboratory fault that separates different materials shows distinct directionality in both rupture speeds and rupture modes. The rupture in the positive direction with respect to the fault is always crack-like growing at the Generalized Rayleigh (GR) wave speed. However, in the negative direction both stable and unstable slip pulses are observed. Higher load and thinner LVZ facilitate the unstable slip pulses. The trailing tip for both types of pulses propagates at the GR wave speed, the leading tip of the stable pulse propagates with the GR wave speed while that of the unstable pulse features a supershear speed.

© 2021 Elsevier Ltd. All rights reserved.

## 1. Introduction

Geological fault is a complicated structure characterized by a damage zone or a low velocity zone (LVZ) embedded in host rocks [1–4]. The damage zone or the low velocity zone (LVZ), which may be induced by aseismic processes [5–7] or coseismic processes [8,9], may have profound influences on the rupture characteristics [10–14].

Using the finite difference method with slip-weakening law [15,16], Harris and Day [10] pioneered systematic study of the effects of LVZ on earthquake rupturing characteristics. They studied three fault configurations (FC): FC1 - fault bisecting a finite LVZ, FC2 - fault on the edge of a finite LVZ, and FC3 - fault on the edge of an infinite LVZ (i.e., bimaterial fault). They observed high frequency oscillations of the slip function due to the finite LVZ in both the positive direction and the negative direction with respect to the fault (the positive direction is the same direction as the slip direction of the more compliant material) for both FC1 and FC2. Using the finite difference method with a modified Prakash–Clifton friction law that has a constant coefficient of friction [17,18], Ben-Zion and Huang [11] examined the possibility of developing a self-sustained, wrinkle-like pulse (i.e., Heaton pulse [19]) in the positive direction during rupture growth for FC2. Huang and her coworkers carried out systematic studies on

the rupture propagation characteristics for FC1 using the spectrum element method coupled with a modified slip-weakening friction law and a strongly velocity-weakening friction law [12–14]. They showed the formation of the pulse-like rupture and the modulation of the slip function by the LVZ. These numerical studies have revealed interesting features on the effect of LVZ on the rupture velocity and rupture mode.

Carefully designed experiments can be used to validate numerical simulations and further provide conclusive evidence. The laboratory experiments have provided conclusive evidence to the formation of supershear rupture [20]. The directionality of rupture propagation was also observed for FC3, where the LVZ with infinite width is simulated with a low velocity material [21]. Sammis et al. [22] showed the asymmetric rupture propagation for FC3 with the LVZ simulated with a damaged polymer plate using thermal-shock. They also showed that the rupture velocity is always sub-Rayleigh and it decreases with the width of the LVZ for FC1.

The existing numerical and experimental studies on LVZ are focused on FC1 and FC3. For FC2, there are only a few numerical studies in the literature [10,11]. Based on fracture mechanics theory [23], shear ruptures in layer systems tend to propagate along the material interface, corresponding to the case where the damage zone is on one side of the fault [8,9]. However, other scenarios of damage zone distribution have also been observed in nature [24]. This study is intended to experimentally address rupturing characteristics for FC2, where the fault is on the edge of a finite LVZ.

\* Corresponding author at: Department of Civil and Mineral Engineering, University of Toronto, Toronto, ON, Canada M5S 1A4.

E-mail address: [kaiwen.xia@utoronto.ca](mailto:kaiwen.xia@utoronto.ca) (K. Xia).

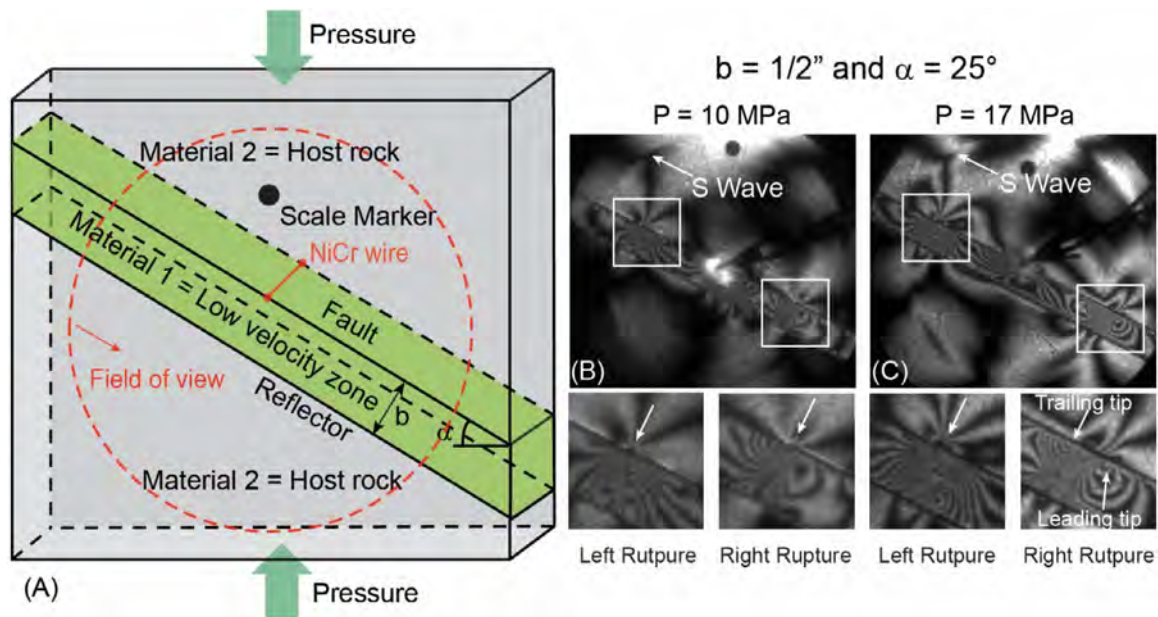


**Fig. 1.** (A) The laboratory fault model FC2 (fault on the edge of a low velocity zone). The width of LVZ is denoted as  $b$ , and the inclination angle  $\alpha$ . The rupture is triggered on the top material interface (which is the fault) at the hypocenter while the other interface acts as the reflector for stress waves emitted from the moving rupture. The black dot in the field of view is a  $1/4''$  (6.35 mm) scale marker. Typical results showing both crack-like ruptures in (B) and in (C). The left rupture is crack-like while the right pulse-like (Hereafter, rupture-tips and tips of the slip pulse characterized by stress singularity are indicated with white arrows in figures).

## 2. Experimental design and typical results

The schematic drawing of laboratory FC2 model is shown in Fig. 1A. The LVZ (Material 1) has a width  $b$  and it is enclosed by the other two identical plates (Material 2) cut out of a  $6''$  by  $6''$  square. The thickness of the plates is  $3/8''$  and thus the problem can be assumed to be plain stress. We use Homalite 100 (Material 2) to simulate the host rock, and Polycarbonate (Material 1) to simulate the low velocity zone. Homalite has a shear wave speed  $C_S^{Fast} = 1200$  m/s and a longitudinal wave speed  $C_P^{Fast} = 2498$  m/s; and Polycarbonate has a shear wave speed  $C_S^{Slow} = 960$  m/s and a longitudinal wave speed  $C_P^{Slow} = 2182$  m/s. The Generalized Rayleigh (GR) wave speed for the material combination  $C_{GR}$  is 959 m/s. The shear wave speed ratio of Homalite to Polycarbonate is  $r_s = 1.25$ . This ratio is close to one of the scenarios studied by Harris and Day [10] for FC2 where  $r_s = 1.2$ . In our experiments the earthquake ruptures were triggered by an exploding wire. The subsequent rupture propagation was visualized using the photoelasticity technique and captured with an ultra-high speed camera [20]. The isochromatic fringe pattern obtained using the photoelasticity method represents the contours of in-plane shear stresses.

## 3. Experimental results

### 3.1. Crack-like and pulse-like ruptures

With respect to the fault, the propagation direction of the left ruptures is positive and that of the right ruptures negative [25]. Typical results are shown in Fig. 1B and C. To better visualize the stress field around the rupture-tip from the LVZ side, the width of the LVZ in these two tests is  $1/2''$ . We can see that for both cases the stress fields near the left rupture are very similar, exhibiting a clear singular point characterized by a caustic spot, which is the rupture-tip. These two ruptures are obviously crack-like. On the contrary, the stress fields of the two right ruptures are very different. The right rupture in Fig. 1B is crack-like as evidenced by the caustic spot, while the right rupture in Fig. 2C does not have

clear singularity on the host rock side. As we can see from the LVZ side, there are two singular points in the fringe pattern. We interpret the front point (leading tip) as the boundary between the locked fault zone to its right and sliding fault zone to its left, and the back point (trailing tip) as the boundary between the sliding fault zone to its right and locked fault zone to its left. These two tips enclose a pulse-like rupture, which is consistent with the theoretical model proposed by Rice et al. [8]. The self-healing, propagating slip pulse is reminiscent of Heaton pulse observed in natural earthquakes [19].

### 3.2. Nucleation mechanism of pulse-like ruptures

A few mechanisms have been proposed in the literature for the occurrence of pulse-like ruptures. Rice and his coworkers suggested that assuming certain frictional law of the slip-rate weakening type, pulse-like earthquake faulting is attainable [26]. In addition to the nature of frictional laws, geometrical effects are also thought to govern the occurrence of pulse modes of rupture. In particular some researchers [27] believe that spatial stress and frictional heterogeneities (e.g., asperity distribution) promote slip pulse formation. Besides, the existence of bimaterial contrast is a candidate for the genesis of pulses [28]. Finally, the low velocity zone may also nucleate slip pulse based on numerical simulation (13,14). Experimentally Lykotrafitis et al. [29] provided the first evidence of the pulse-like rupture along homogeneous frictional contact driven by impact loading. Lu et al. [30] then demonstrated such pulse-like rupture along homogeneous faults in laboratory earthquakes with proper interfacial roughness.

The experiments proposed here are primarily aimed towards the study of the mechanically triggered rather than the heterogeneity or frictional law caused slip pulses. In the current study, there are three controlling parameters:  $b$  - the width of LVZ,  $\alpha$  - the inclination angle of LVZ, and  $P$  - the uniaxial pressure applied. When the fault ruptures, elastic waves are emitted from the rupture-tip and are reflected at reflector - the other interface between the LVZ and the host rock [11]. The slip direction carried by the wave is the same as the slip direction at the rupture-tip

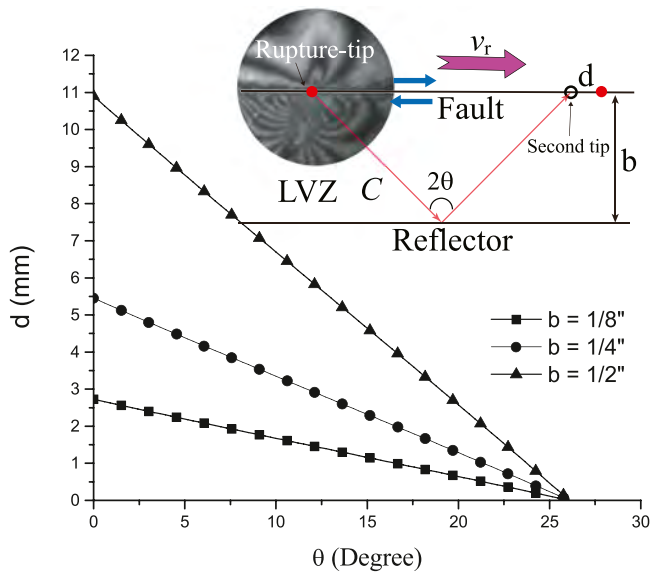


**Fig. 2.** Distance between the rupture-tip and the arrival location of the stress wave. The inset shows the mechanism controlling the nucleation of the pulse-like rupture. For rays with angle smaller than  $26^\circ$ , the stress wave arrives behind the rupture-tip for all LVZ widths studied in this work. These rays cause dynamic compression of the fault and thus may lead to the pulse-like rupture.

and only the magnitude is reduced after reflection. When this reflected wave arrived at the fault plane, it caused oscillation of the slip function both in the positive and negative directions as identified by numerical simulations [10–14]. Furthermore, the interaction of the reflected wave with the fault also leads to dynamic compression or dynamic tension due to the existence of the material contrast [28,31,32].

The nucleation mechanism of the pulse-like rupture in the negative direction of a fault with LVZ is illustrated in the inset of Fig. 2. The rupture-tip indicated by a dot propagates in the negative direction at velocity  $v_r$  to a new position. During the meantime, the elastic wave emitted by the rupture with velocity  $C$  is reflected at the reflector. The isochromatic fringe pattern around the bimaterial rupture-tip is taken from reference [21]. One representative path of the elastic wave is plotted, and the wave arrives at the fault indicated by a small circle after reflection. The rupturing along the bimaterial interface leads to both shear and compressive normal stresses. First the shear stress is considered. The slip carried by the stress wave due to shear interacts with the bimaterial fault after reflection, leading to

dynamic compression [25]. Further the rupture along the bimaterial fault induces dynamic compression. This compression is carried by the stress wave and got reflected to the fault with reduced magnitude. Dynamic compressive loadings due to these two mechanisms may heal the fault at the circle, leading to a pulse-like rupture eventually. In the positive direction, these interactions induce tension and thus healing (therefore the slip pulse) is not possible.

As shown in Fig. 2,  $\theta$  is the angle between the ray of the elastic wave and the normal direction of the fault. The distance between the rupture-tip (second dot) and the arrival location of the ray (circle) is  $d = 2b(v_r/C - \sin\theta)/\cos\theta$ . Taking  $C$  as  $C_p^{Slow} = 2182$  m/s and  $v_r$  as  $C_{GR} = 959$  m/s, we can plot  $d$  as a function of the angle  $\theta$  in Fig. 2. For all three LVZ widths considered in this study, stress wave rays with angle smaller than  $26^\circ$  arrive at the fault after the rupture-tip. These rays will contribute to the healing of the fault after the rupture-tip. The reflector is thus the geometrical reason for the nucleation of the slip pulse and thus the property of the pulse is controlled by the material contrasts and the frictional properties of the interface. This observation is consistent with the results by Huang and her coworkers in their study of the slip pulses for FC1 [12,13].

### 3.3. Effect of loading on the rupture modes in the negative direction

In Fig. 3, experimental results featuring  $b = 1/8''$  and  $\alpha = 25^\circ$  are shown to illustrate the effect of loading on the slip pulse. In Fig. 3A, both left and right ruptures are crack-like; in Fig. 3B and C, the left ruptures are crack-like while the right ones are pulse-like. It can be concluded that higher uniaxial loading facilitates the nucleation of pulse-like rupture in the negative direction.

### 3.4. Stable pulse-like rupture

Fig. 4 demonstrates the formation and growth of a slip pulse using the rupture-tip history. The inter-frame time is  $3 \mu s$  and the first frame corresponds to  $38 \mu s$  after triggering. As seen from the figures, the rupture in the positive direction (left) is always  $+C_{GR}$ . However, the rupture in the negative direction shows a transition from a crack-like rupture to a pulse-like at  $44 \mu s$ . After  $47 \mu s$ , the length of the slip pulse is roughly a constant ( $\sim 4.6$  mm) and this type of pulse is called a stable pulse. Both the leading tip and the trailing tip of the pulse propagate at  $-C_{GR}$ .

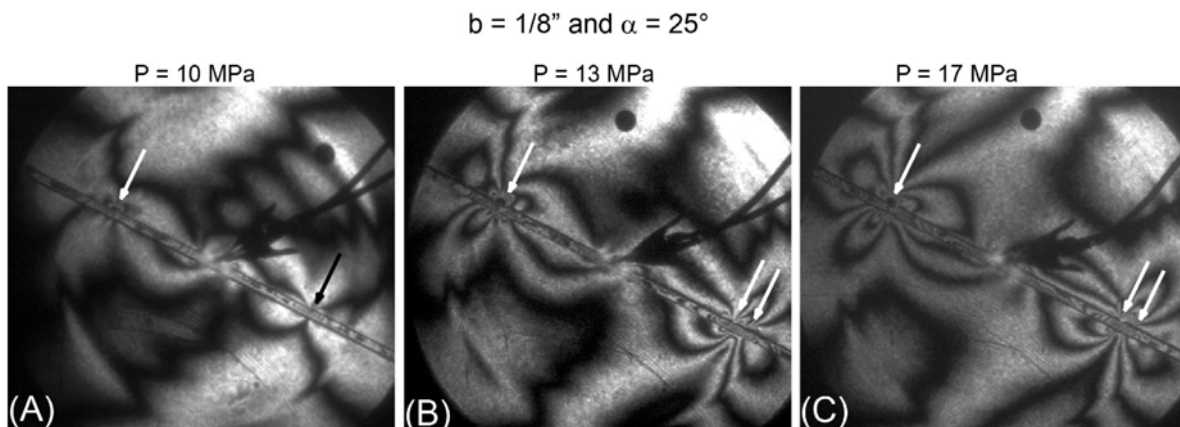


**Fig. 3.** The effect of far-field loading on the nucleation of pulse-like rupture in the negative direction.

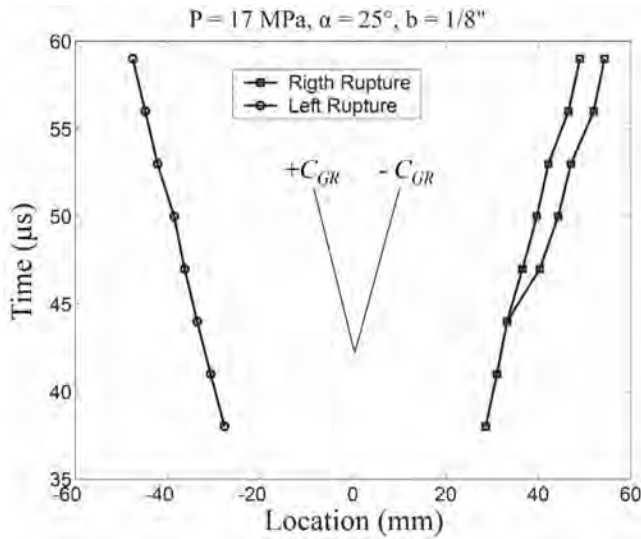


Fig. 4. The rupture-tip history of a stable slip pulse.

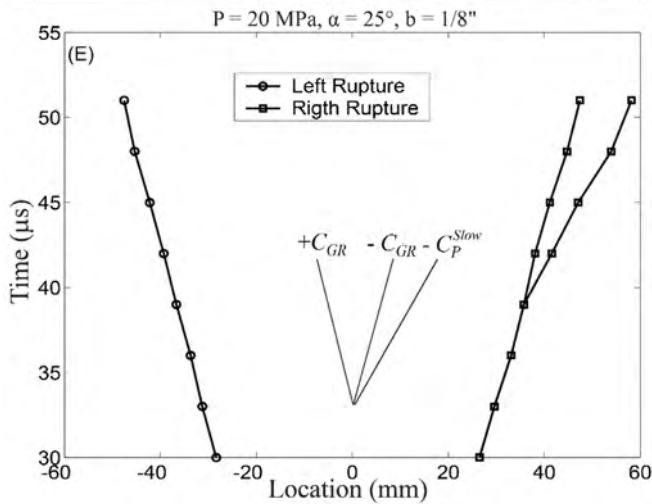
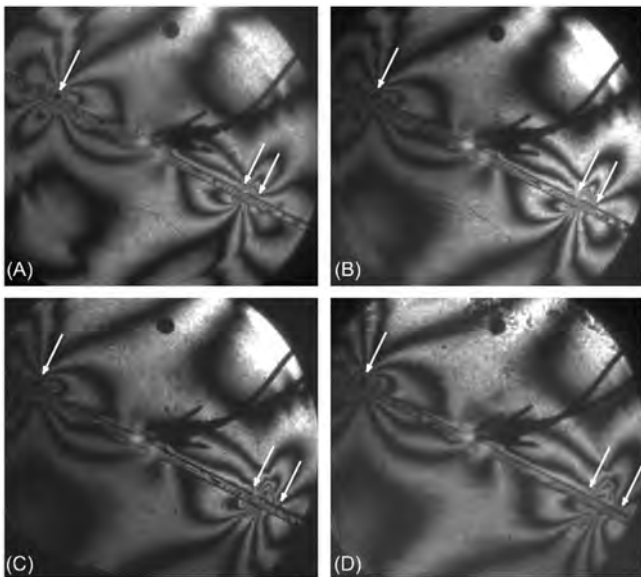


Fig. 5. Photograph sequence from one experiment with unstable pulse: (A) 42  $\mu$ s, (B) 45  $\mu$ s, (C) 48  $\mu$ s, (D) 52  $\mu$ s. (E) The rupture-tip history of this test.

Table 1

Summary of experimental results. The left rupture speed is always  $+C_{GR}$ , while the right rupture is either crack-like or pulse-like. For the pulse-like right rupture, the velocity of the trailing tip is always  $-C_{GR}$ , velocity shown in the table is for the leading tip.

$\alpha$ ( $^\circ$ )	$b$ ( $''$ )	$P$ (MPa)	Mode	Velocity of left rupture	Velocity of right rupture
25	1/8	20	Pulse	$+C_{GR}$	$-C_P^{Slow}$
25	1/8	17	Pulse	$+C_{GR}$	$-C_{GR}$
25	1/8	13	Crack	$+C_{GR}$	$-C_{GR}$
25	1/4	17	Pulse	$+C_{GR}$	$-C_{GR}$
25	1/4	13	Crack	$+C_{GR}$	$-C_{GR}$
25	1/2	17	Pulse	$+C_{GR}$	$-C_{GR}$
25	1/2	10	Crack	$+C_{GR}$	$-C_{GR}$
22.5	1/8	17	Pulse	$+C_{GR}$	$-C_{GR}$
22.5	1/8	13	Crack	$+C_{GR}$	$-C_{GR}$
22.5	1/4	17	Crack	$+C_{GR}$	$-C_{GR}$
22.5	1/4	13	Crack	$+C_{GR}$	$-C_{GR}$
20	1/2	13	Crack	$+C_{GR}$	$-C_{GR}$
20	1/4	13	Crack	$+C_{GR}$	$-C_{GR}$
20	1/8	13	Crack	$+C_{GR}$	$-C_{GR}$

### 3.5. Unstable pulse-like rupture

In Fig. 5, we present a time sequence of photographs of an experiment with  $P = 20$  MPa,  $\alpha = 25^\circ$  and  $b = 1/8''$  along with its rupture-tip history plot. The left rupture is always crack-like and grows at  $+C_{GR}$ . The right rupture on the other hand starts as crack-like and soon develops into pulse-like. From Fig. 5A-D, the length of the pulse increases with time. This fact can be seen clearly from Fig. 5E. The trailing tip of the pulse propagate at  $-C_{GR}$  while the leading tip of the pulse assumes velocity  $-C_P^{Slow}$  right after its birth. This unstable slip pulse is somewhat similar to that in the homogeneous fault system as reported by Lu et al. [30] based on the measurement of near fault slip history.

There are also some similarities between rupture characteristics in the current case and those observed in bimaterial fault ruptures [21], where a rupture moving in the negative direction can transition to a supershear speed close to  $-C_P^{Slow}$ . Since we have not observed this unstable pulse phenomena for experiments with lower pressure, it seems that there exists a critical pressure for a given LVZ width  $b$  and an inclination angle  $\alpha$ , beyond which the leading tip of the slip pulse propagates at a supershear speed right. Finally, the experimental results are summarized in Table 1. One can see that higher load and thinner LVZ facilitate pulse-like ruptures in the negative direction.

## 4. Discussion and implications

There are some similarities between our results and those reported by Harris and Day [10] for the case  $r_s = 1.2$ , when the generalized Rayleigh wave speed can be defined. The numerical result predicted that the rupture moving in the positive direction features a speed close to  $+C_{GR}$ , which is consistent with our experimental results. Along the negative direction, both their numerical simulation and our experiment show that the supershear ruptures are possible. The supershear rupture velocity in both studies consistently points to the P wave speed of the slower LVZ material. However we observed pulse-like ruptures, while they only reported the occurrence of crack-like supershear rupture in the negative direction. As compared with the numerical work by Ben-Zion and Huang [11], the experimentally observed propagation direction of the pulse-like rupture is opposite to what they proposed.

The modulus of Homalite is about 5 GPa and that of the crustal rock is around 50 GPa. Therefore, the load in the laboratory ( $P \sim 15$  MPa) can be scaled up to at least 150 MPa ( $\sim 5$  km depth) in the field, which is close to what is expected at the seismogenic

depth. We assume that the frictional property is material independent and thus  $L/dc$  is a constant, where  $L$  is the length of the slip pulse. Because the critical slip distance in the field is around 0.5 m and that in the lab is around 20  $\mu\text{m}$  [20]. The length of the pulse in the laboratory for the stable slip pulse (4.6 mm) can be scaled to the field condition as 1.15 km. This length lies in the range of pulse length for real earthquakes (0.8 km  $\sim$  13 km) as reported by Heaton [19].

## 5. Conclusion

We experimentally studied the effect of low velocity zone (LVD) on earthquake ruptures. The directionality of both rupture speeds and rupture modes were observed. The rupture growth in the positive direction is always crack-like with the generalized Rayleigh (GR) wave speed. Due to the existence of the reflector, the rupture in the negative direction may become pulse-like as facilitated by higher loading level and thinner LVD. This is an alternative nucleation mechanism of pulse-like earthquake ruptures. The pulse-like rupture is usually stable with both the leading tip and the trailing tip propagating at the GR wave speed. However, under sufficiently high loading, the pulse-like rupture may become unstable with its leading tip propagating at supershear speed while trailing tip at GR wave speed.

## CRediT authorship contribution statement

**Kaiwen Xia:** Conducted the experiments, Data analysis, Manuscript was drafted, Manuscript was edited. **Ares J. Rosakis:** Supervised the study, Manuscript was edited.

## Declaration of competing interest

The authors declare that they have no known competing financial interests or personal relationships that could have appeared to influence the work reported in this paper.

## Data availability

All data is available in the main text.

## Acknowledgments

This study was supported by the National Key R&D Program of China [#2018YFC1503302], and the Natural Science Foundation of Tianjin [#19JCZDJC40400]. K.X. was partially supported by the Natural Sciences and Engineering Research Council of Canada (NSERC) through the Discovery Grant [#72031326].

## References

- Y. Ben-Zion, C.G. Sammis, Characterization of fault zones, *Pure Appl. Geophys.* 160 (2003) 677–715, <http://dx.doi.org/10.1007/PL00012554>.
- F.M. Chester, J.S. Chester, Ultracataclastic structure and friction processes of the punchbowl fault, San Andreas system, California, *Tectonophysics* 295 (1998) 199–221, [http://dx.doi.org/10.1016/S0040-1951\(98\)00121-8](http://dx.doi.org/10.1016/S0040-1951(98)00121-8).
- R.H. Sibson, Brecciation processes in fault zones: Inferences from earthquake rupturing, *Pure Appl. Geophys.* 124 (1986) 159–175, <http://dx.doi.org/10.1007/bf00875724>.
- C.H. Scholz, Wear and gouge formation in brittle faulting, *Geology* 15 (1987) 493–495, [http://dx.doi.org/10.1130/0091-7613\(1987\)15](http://dx.doi.org/10.1130/0091-7613(1987)15).
- C. Childs, T. Manzocchi, J.J. Walsh, C.G. Bonson, A. Nicol, M.P.J. Schöpfer, A geometric model of fault zone and fault rock thickness variations, *J. Struct. Geol.* 31 (2009) 117–127, <http://dx.doi.org/10.1016/j.jsg.2008.08.009>.
- F.M. Chester, J.S. Chester, Stress and deformation along wavy frictional faults, *J. Geophys. Res.: Solid Earth* 105 (2000) 23421–23430, <http://dx.doi.org/10.1029/2000jb900241>.
- P.A. Cowie, C.H. Scholz, Physical explanation for the displacement-length relationship of faults using a post-yield fracture mechanics model, *J. Struct. Geol.* 14 (1992) 1133–1148, [http://dx.doi.org/10.1016/0191-8141\(92\)90065-5](http://dx.doi.org/10.1016/0191-8141(92)90065-5).
- J.R. Rice, C.G. Sammis, R. Parsons, Off-fault secondary failure induced by a dynamic slip pulse, *Bull. Seismol. Soc. Am.* 95 (2005) 109–134, <http://dx.doi.org/10.1785/0120030166>.
- S.Q. Xu, Y. Ben-Zion, Theoretical constraints on dynamic pulverization of fault zone rocks, *Geophys. J. Int.* 209 (2017) 282–296, <http://dx.doi.org/10.1093/gji/ggx033>.
- R.A. Harris, S.M. Day, Effects of a low-velocity zone on a dynamic rupture, *Bull. Seismol. Soc. Am.* 87 (1997) 1267–1280.
- Y. Ben-Zion, Y.Q. Huang, Dynamic rupture on an interface between a compliant fault zone layer and a stiffer surrounding solid, *J. Geophys. Res.: Solid Earth* 107 (2002) ESE 6–1–ESE 6–13, <http://dx.doi.org/10.1029/2001JB000254>.
- Y.H. Huang, J.P. Ampuero, D.V. Helmlinger, The potential for supershear earthquakes in damaged fault zones – theory and observations, *Earth Planet. Sci. Lett.* 433 (2016) 109–115, <http://dx.doi.org/10.1016/j.epsl.2015.10.046>.
- Y.H. Huang, J.P. Ampuero, Pulse-like ruptures induced by low-velocity fault zones, *J. Geophys. Res.: Solid Earth* 116 (2011) <http://dx.doi.org/10.1029/2011jb008684>.
- Y.H. Huang, J.P. Ampuero, D.V. Helmlinger, Earthquake ruptures modulated by waves in damaged fault zones, *J. Geophys. Res.: Solid Earth* 119 (2014) 3133–3154, <http://dx.doi.org/10.1002/2013jb010724>.
- Y. Ida, Cohesive force across tip of a longitudinal-shear crack and Griffiths specific surface-energy, *J. Geophys. Res.* 77 (1972) 3796–3805, <http://dx.doi.org/10.1029/JB077i020p03796>.
- A.C. Palmer, J.R. Rice, The growth of slip surfaces in the progressive failure of over-consolidated clay, *Proc. R. Soc. A* 332 (1973) 527–548, <http://dx.doi.org/10.1098/rspa.1973.0040>.
- V. Prakash, A pressure-shear plate impact experiment for investigating transient friction, *Exp. Mech.* 35 (1995) 329–336, <http://dx.doi.org/10.1007/BF02317542>.
- V. Prakash, Time-resolved friction with applications to high-speed machining: Experimental observations, *Tribol. Trans.* 41 (1998) 189–198, <http://dx.doi.org/10.1080/10402009808983738>.
- T.H. Heaton, Evidence for and implications of self-healing pulses of slip in earthquake rupture, *Phys. Earth Planet. Inter.* 64 (1990) 1–20, [http://dx.doi.org/10.1016/0031-9201\(90\)90002-F](http://dx.doi.org/10.1016/0031-9201(90)90002-F).
- K.W. Xia, A.J. Rosakis, H. Kanamori, Laboratory earthquakes: the sub-Rayleigh-to-supershear rupture transition, *Science* 303 (2004) 1859–1861, <http://dx.doi.org/10.1126/science.1094022>.
- K. Xia, A.J. Rosakis, H. Kanamori, J.R. Rice, Laboratory earthquakes along inhomogeneous faults: directionality and supershear, *Science* 308 (2005) 681–684, <http://dx.doi.org/10.1126/science.1108193>.
- C.G. Sammis, A.J. Rosakis, H.S. Bhat, Effects of off-fault damage on earthquake rupture propagation: Experimental studies, *Pure Appl. Geophys.* 166 (2009) 1629–1648, <http://dx.doi.org/10.1007/s00024-009-0512-3>.
- J.W. Hutchinson, Z. Suo, Mixed-mode cracking in layered materials, *Adv. Appl. Mech.* 29 (1992) 63–191, [http://dx.doi.org/10.1016/S0065-2156\(08\)70164-9](http://dx.doi.org/10.1016/S0065-2156(08)70164-9).
- Yihe Huang, Earthquake rupture in fault zones with along-strike material heterogeneity, *J. Geophys. Res.: Solid Earth* 123 (2018) 9884–9898, <http://dx.doi.org/10.1029/2018jb016354>.
- A. Cochard, J.R. Rice, Fault rupture between dissimilar materials: Ill-posedness, regularization, and slip-pulse response, *J. Geophys. Res.: Solid Earth* 105 (2000) 25891–25907, <http://dx.doi.org/10.1029/2000jb900230>.
- G. Zheng, J.R. Rice, Conditions under which velocity-weakening friction allows a self-healing versus a cracklike mode of rupture, *Bull. Seismol. Soc. Am.* 88 (1998) 1466–1483.
- S.B. Nielsen, J.M. Carlson, K.B. Olsen, Influence of friction and fault geometry on earthquake rupture, *J. Geophys. Res.: Solid Earth* 105 (2000) 6069–6088, <http://dx.doi.org/10.1029/1999JB900350>.
- Y. Ben-Zion, Dynamic ruptures in recent models of earthquake faults, *J. Mech. Phys. Solids* 49 (2001) 2209–2244.
- G. Lykotrafitis, A.J. Rosakis, G. Ravichandran, Self-healing pulse-like shear ruptures in the laboratory, *Science* 313 (2006) 1765–1768, <http://dx.doi.org/10.1126/science.1128359>.
- X. Lu, N. Lapusta, A.J. Rosakis, Pulse-like and crack-like ruptures in experiments mimicking crustal earthquakes, *Proc. Natl. Acad. Sci. USA* 104 (2007) 18931–18936, <http://dx.doi.org/10.1073/pnas.0704268104>.
- K. Ranjith, Slip dynamics at an interface between dissimilar materials, *J. Mech. Phys. Solids* 49 (2001) 341–361, [http://dx.doi.org/10.1016/s0022-5096\(00\)00029-6](http://dx.doi.org/10.1016/s0022-5096(00)00029-6).
- J. Weertman, Unstable slippage across a fault that separates elastic media of different elastic-constants, *J. Geophys. Res.: Solid Earth* 85 (1980) 1455–1461, <http://dx.doi.org/10.1029/JB085iB03p01455>.